Nanoscale Advances

ROYAL SOCIETY OF CHEMISTRY

PAPER

View Article Online
View Journal | View Issue

Open Access Article. Published on 18 December 2024. Downloaded on 1/21/2026 1:24:38 AM.
This article is licensed under a Creative Commons Attribution-NonCommercial 3.0 Unported Licence.

Check for updates

Cite this: *Nanoscale Adv.*, 2025, **7**, 1091

An economical synthesis of benzodiazepines using ACT@IRMOF core–shell as a potential eco-friendly catalyst through the activated carbon of thymus plant (ACT)†

Maryam Fereydooni,[a] Ramin Ghorbani-Vaghei *[ab] and Sedigheh Alavinia[a]

Received 4th November 2024
Accepted 15th December 2024

DOI: 10.1039/d4na00907j

rsc.li/nanoscale-advances

Here, a straightforward design is employed to synthesize a nanocatalyst based on a carbon-activated modified metal–organic framework using the solvothermal method. This work presents a simple and practical approach for producing the activated carbon derived from the Thymus plant (ACT) modified with amine-functionalized isoreticular metal–organic framework-3 (IRMOF-3) to create an ACT@IRMOF-3 core–shell structure. Successful functionalization was confirmed through N_2 adsorption isotherms, FT-IR, FE-SEM, TEM, EDS, elemental mapping, TGA, and XRD analysis. The ACT@IRMOF-3 nanocomposite demonstrated exceptional performance in the synthesis of novel benzodiazepine derivatives, facilitating high product yields using various 1,2-phenylenediamine and aromatic aldehydes under mild conditions. The obtained results demonstrated that the presence of IRMOF-3 on the surface of ACT remarkably increases the catalytic reaction yield. The present methodology offers several merits such as high catalytic activity, excellent yields, short reaction times, cleaner reactions, simple operations, and compatibility of a wide range of substrates. Furthermore, the catalyst can be easily isolated from the reaction mixture *via* filtration and retains remarkable reusability and catalytic activity even after six consecutive reaction cycles.

Introduction

There is a wide range of compounds in which benzodiazepine serves as an important structural component, including various biologically active pharmaceutical ingredients and natural products.[1] Benzodiazepines exhibit diverse biological properties such as sedative, hypnotic, anxiolytic, anticonvulsant, and muscle relaxant properties, making them valuable in various therapeutic applications (Fig. 1).[2,3] Furthermore, these compounds have been extensively studied for their role in central nervous system disorders, including anxiety, epilepsy, and insomnia. Benzodiazepine derivatives, like 1,4-benzodiazepines, have been crucial in drug development for conditions such as AIDS, cancer, and antiviral treatment.[4] Overall, the study of benzodiazepines and related heterocyclic compounds continues to be a vital area of research in medicinal chemistry, offering potential advancements in the development of new therapeutic agents.

Recently, researchers have focused on synthesizing these derivatives with enhanced biological activities through strategic substitutions and innovative synthesis methods. Continuous flow synthesis has been described for six benzodiazepines from aminobenzophenones, including diazepam and clonazepam.[5] One-step synthesis of pyrido-benzodiazepine backbones and analogs was achieved by ring-opening hydrolysis and C–H bond activation.[6] In addition, the synthesis of 1,4-benzodiazepines using a palladium catalyst was discussed, highlighting various reactions and catalytic processes for their efficient preparation.[7] Multicomponent reactions, especially Ugi and Mannich-type reactions, provide efficient and sustainable methods for the synthesis of benzodiazepines with diverse biological activities, providing novel therapeutic candidates through one-pot protocols.[8] Considering the broad medicinal and biological applications of benzodiazepine derivatives, synthetic chemists face a significant challenge in providing newer and more efficient catalytic systems compatible with green chemistry principles for synthesizing these compounds.

Metal–organic frameworks (MOFs) exhibit significant potential in catalysis due to their diverse structures and properties.[3] MOFs can act as Lewis acid–base catalysts, with frustrated Lewis acid–base pairs (FLPs) or bifunctional solid catalysts capable of activating molecular hydrogen.[9] These structures offer well-defined porosity, controllable morphology,

[a]*Department of Organic Chemistry, Faculty of Chemistry and Petroleum Sciences, Bu-Ali Sina University, 6517838683, Hamadan, Iran. E-mail: rgvaghei@yahoo.com; ghorbani@basu.ac.ir*

[b]*Department of Organic Chemistry, Faculty of Chemistry, University of Guilan, Rasht, Iran*

† Electronic supplementary information (ESI) available. See DOI: https://doi.org/10.1039/d4na00907j

© 2025 The Author(s). Published by the Royal Society of Chemistry

Open Access Article. Published on 18 December 2024. Downloaded on 1/21/2026 1:24:38 AM.
This article is licensed under a Creative Commons Attribution-NonCommercial 3.0 Unported Licence.

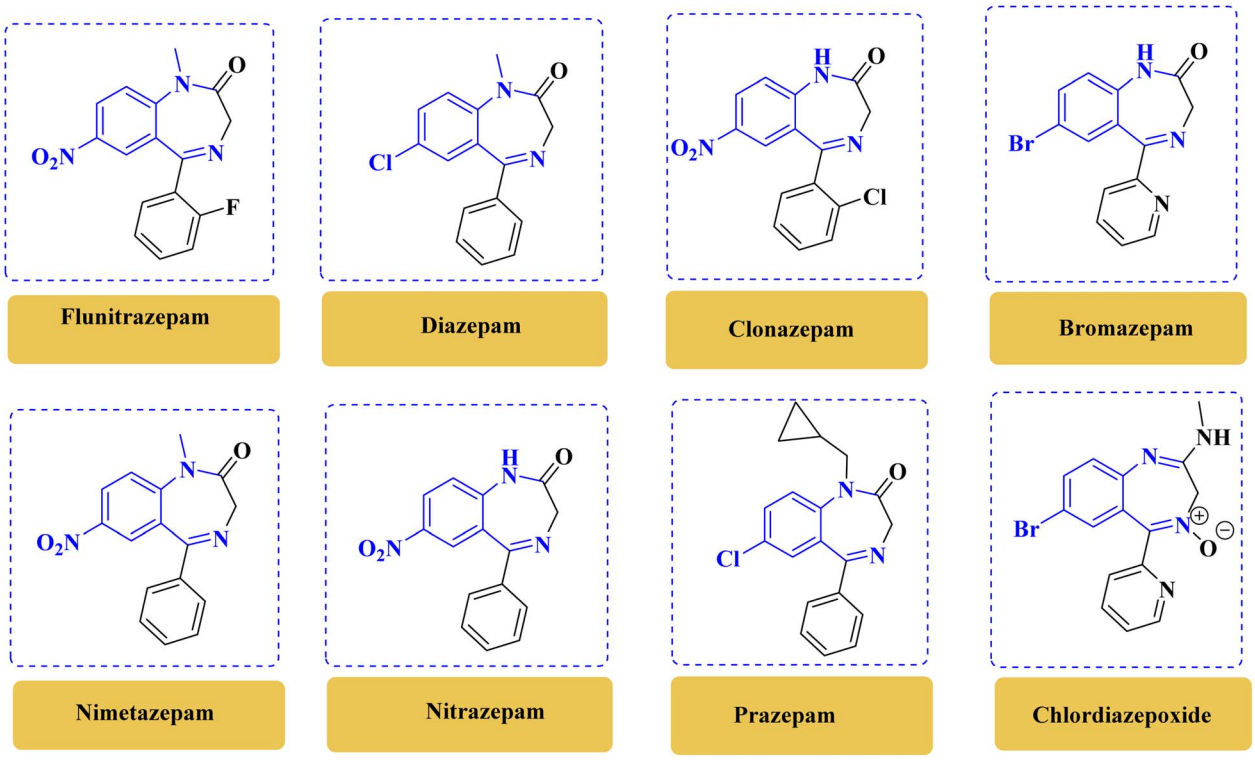

Fig. 1 Chemical structure of benzodiazepines with biological activity.[1–4]

and the ability to support nanomaterials, enhancing their catalytic applications.[10] To improve catalytic efficiency, MOFs can be functionalized or integrated with other materials to create composites or hybrids, expanding their active sites and stability.[10–12] Additionally, modifications to MOFs can enhance catalytic activity without changing their chemical nature, making them versatile catalysts for various reactions.[12] Though, these materials are time-consuming and costly, which limits their utilization in practice.

Recently, activated carbon/MOF nanocomposites represent a versatile platform for catalytic reactions, showing great potential in advancing organic chemistry and environmental remediation.[13–16] Carbon-based nanocomposites, including graphene, carbon nanotubes, and activated carbon, are extensively utilized in various applications[17] The application of activated carbon and its composites is a crucial aspect in various industries due to the unique properties it possesses.[18] Activated carbon is known for its exceptional adsorption capabilities, high surface area, porous structure, and high chemical/thermal stability making it an excellent choice for designing carbon-based nanocatalyst.[19] In recent years, activated carbon derived from natural sources and biomass such as coconut shells and wood has gained popularity for its environmental and sustainable nature.[19–26] Activated carbon, which is derived from natural materials, plays a crucial role in various organic reactions.[27–31] Consequently, the development and surface modification of activated carbon-based nanocatalysts from natural materials is a straightforward, cost-effective, and green approach for the synthesis of *N*-containing heterocyclic compounds.[15–18,25]

Enthused by the aforementioned findings, in this work, activated carbon derived from the Thymus plant (ACT) has been successfully modified with IRMOF-3 (ACT@IRMOF-3) for the synthesis of benzodiazepine. Given that activated carbon has a smaller surface area compared to IRMOF-3 nanoparticles, incorporating a small number of IRMOF-3 nanoparticles can significantly increase the surface area created in ACT@IRMOF-3 core–shell structure. Furthermore, the synthesized ACT@IRMOF-3 nanocomposite is a cost-effective nanocatalyst as it mainly consists of carbon derived from waste materials. The combination of IRMOF-3 with Thymus-activated carbon enhances catalytic efficiency and selectivity, offering a platform for the development of carbon-based multifunctional catalysts. By integrating the benefits of activated carbon surface modification capabilities with the high surface area and multifunctionality of IRMOF-3, this catalyst provides a unique approach to benzodiazepine synthesis. Each nanocomposite component contributes to a synergistic effect, acting as a Lewis acid and enhancing catalytic efficiency.

Experimental

Materials

Zinc nitrate hexahydrate [$Zn(NO_3)_3 \cdot 6H_2O$] was utilized as the metal source to synthesize IRMOF-3 MOFs (procured from Merck Co., Germany) with a purity of 99%. 2-Aminotherephthalic acid (NH_2BDC, 98%), phosphoric acid (85%), dimedone (98%), 1,2-phenylenediamine (99.5%), *N*,*N*-dimethylformamide (DMF) (anhydrous) were obtained from Aldrich

 © 2025 The Author(s). Published by the Royal Society of Chemistry

Open Access Article. Published on 18 December 2024. Downloaded on 1/21/2026 1:24:38 AM.
This article is licensed under a Creative Commons Attribution-NonCommercial 3.0 Unported Licence.

Co. Zataria multiflora (Thymes) is a culinary herb comprising the dehydrated aerial portions of select plant species within the Thymus genus of flowering plants belonging to the Lamiaceae mint family.

Synthesis of activated carbon derived from thymus plant (ACT)

The ACT was synthesized through the activation, and paralyzing process.[26]

Synthesis of IRMOF-3 (ACT@IRMOF-3) by activated carbon derived from thymus plant (ACT)

The ACT@IRMOF-3 nanocomposite was synthesized using the solvothermal method. Initially, a mixture of 1 g of synthesized ACT, 1.8 g of $Zn(NO_3)_2 \cdot 6H_2O$, and 0.375 g of 2-amino-therephthalic acid was magnetically stirred in a 100 mL vial at room temperature for 1 hour. Subsequently, the solution was transferred to a Teflon-lined autoclave and maintained at 120 °C for 24 h.

The sample was immersed in 10 mL of hot EtOH and 10 mL of DMF for 24 hours to remove any residual trapped acids inside the pores. Subsequently, it was filtered and dried at 100 °C overnight to obtain the ACT@IRMOF-3 nanocomposite (Fig. 2).

The benzodiazepines synthesis

A mixture of benzaldehyde (1 mmol), 1,2-phenylenediamine (1 mmol), dimedone (1 mmol), and ACT@IRMOF-3 (5 mg) in 2 mL solvent of ethanol was stirred at reflux conditions. The reaction progress was checked by TLC (*n*-hexan : ethyl acetate, 2 : 1). After the reaction completion, the mixture was cooled and then centrifuged to separate the catalyst. After drying, the sediment was washed with EtOH (5 mL) to gain the product (Scheme 1).

Result and discussion

Catalyst characterization

Fig. 3 demonstrations the FT-IR absorption spectra spectrum of ACT and ACT@IRMOF-3 nanocomposite. The FT-IR spectrum of ACT shows the existence of an integration band at 3450 cm^{-1} which can be tuned to O–H elongation convulsions of surface hydroxyl groups and some water molecules adsorbed. The integration band at 1615 cm^{-1} is tuned to the C=C elongation pulsations specific to the aromatic structure. Additionally, the strip at 1099 cm^{-1} can be tuned to the O–H curvature or the C–O elongation pulse of phenol, while the strip at 1448 cm^{-1} is tuned to the O–C=O groups (Fig. 3a). FT-IR analysis of the ACT@IRMOF-3 catalyst shows mobile mutations due to the addition of IRMOF-3. An increase in the integration strip to

Fig. 2 The process of ACT@IRMOF-3 core–shell fabrication.

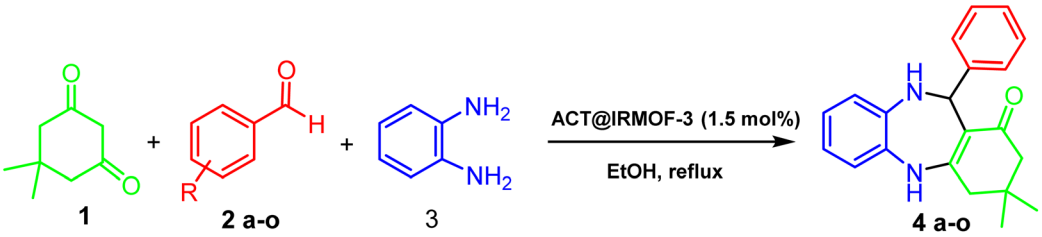

Scheme 1 The procedure for the one-pot synthesis of benzodiazepine derivatives using ACT@IRMOF-3 nanocomposite.

Open Access Article. Published on 18 December 2024. Downloaded on 1/21/2026 1:24:38 AM.
This article is licensed under a Creative Commons Attribution-NonCommercial 3.0 Unported Licence.

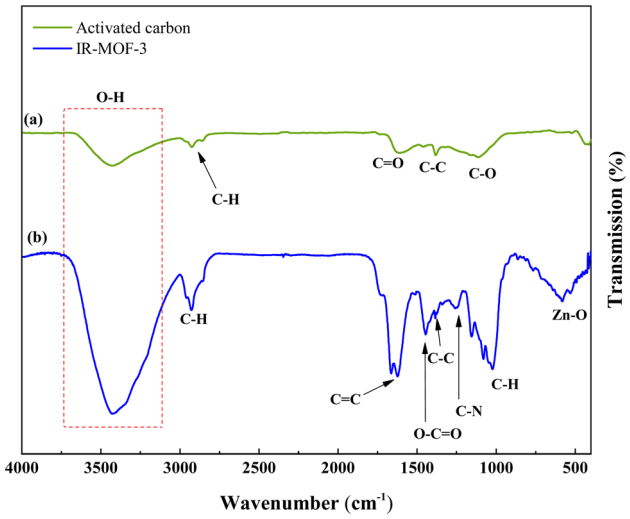

Fig. 3 FTIR spectrum of ACT (a) and ACT@IRMOF-3 nanocomposite (b).

3396 cm^{-1} highlights the presence of carboxylic acid groups of IRMOF-3 adsorbed during modification. A new integration band observed at 595 cm^{-1} is granted to the Zn–O bond of the IRMOF-3 group. An asymmetric strip at 1023 cm^{-1} and a symmetric strip at 1259 cm^{-1} are tuned to the C–O and C–N bond. The bands at about 1448, 1615, and 2915 cm^{-1} are related to O–C=O, C=C, and C–H bonds of ACT@IRMOF-3 (Fig. 3b).

The crystallinity of ACT and ACT@IRMOF-3 nanocomposite were evaluated using X-ray diffraction (Fig. 4). XRD is a noninvasive analytical method that gives thorough evidence regarding the crystalline structure and chemical composition of the material. The XRD pattern for the ACT and ACT@IRMOF-3 nanocomposite demonstrated two main diffraction peaks shown at 24.29° and 43.54° are observed in the 2θ range from 10 to 90° corresponding to *hkl* plane of (100) and (002), respectively, which are the characteristic peaks of activated carbon,

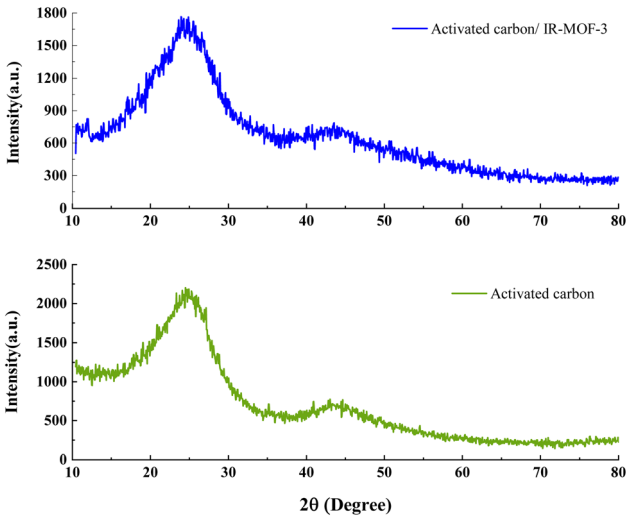

Fig. 4 XRD pattern of ACT and ACT@IRMOF-3.

characteristic of the accumulation composition of the aromatic carbon layers. Additionally, the existence of unidentified particles in the carbon structure shows the existence of various minerals (Fig. 4). The synthesized materials have a semi-crystalline nature. XRD spectrum of ACT@IRMOF-3 confirms the successful integration and modification of ACT with IRMOF-3 particles. From XRD analysis, it is clear that there is no specific change in the morphology of the material after modification of activated carbon (ACT). The spectrum of the ACT@IRMOF-3 catalyst indicates a basic structure analogous to that of ACT but with significant variations in pick intensities. It can therefore be concluded that the XRD analysis explained the adsorption and synthesis of IR-MOF-3 on the surface of ACT (Fig. 4).

Fig. 5 displays the FESEM images of the raw material (Thymus), ACT, and ACT@IRMOF-3 core–shell. Fig. 5A provides evidence that the Thymus particles possess a surface that is predominantly smooth and uniform in nature. It can be observed from Fig. 5(B and C) that the ACT surface shows the presence of numerous cavities, indicating that the pore structure expands after the activation procedure. The ACT material showed a three-dimensional network structure. The high-magnification SEM photograph of ACT reveals the microporous surface Fig. 5(B and C). The synthesized IRMOF-3 shows well-dispersed and nearly spherical uniform nanostructures (Fig. 5D).[27] Fig. 5(E and F) reveals an irregular surface, confirming the loading of IRMOF-3 NPs onto the microporous surface of activated carbon of Thymus. The pore size of the sample ACT was mainly concentrated in 10–30 μm Fig. 5(B and C), while the surface of the ACT@IRMOF-3 catalyst clearly shows the catalyst particles are uniformly nanoscale (Fig. 5F).

More intrinsic and clear images were obtained through TEM analysis which has been displayed in Fig. 6A and B. It shows that the IRMOF-3 particles are mostly cubic-shaped and not aggregated, at all. The particle sizes also are quite in agreement with the FE-SEM data. On close observation, a feeble layer can be observed around the particles, which is anticipated to be the ACT modification with IRMOF-3.

The EDS analysis of ACT (Fig. 7a) and ACT@IRMOF-3 (Fig. 7b) provided crucial insights into the surface composition. The chemical composition of ACT is composed mainly of carbon with a mass percentage of 85.9%, but also of oxygen (14.00%) coming from numerous surface oxygen. The weight percentage results of the EDS analysis of both samples show that the main constituent is carbon. The equivalent quantities of carbon, nitrogen, oxygen, and zinc were 73.1, 0.6, 9.3, and 17.0%, respectively, in the ACT@IRMOF-3 (Fig. 7b). The zinc peak presence confirms the successful modification of ACT with IRMOF-3 and the construction of ACT@IRMOF-3. The analysis showed an increase in the elements nitrogen with a weight percentage reaching 0.6 six times.

Elemental mapping analysis of ACT (Fig. 8a) and ACT@IRMOF-3 (Fig. 8b) nanocomposites shows a high density of carbon elements originating from the ACT nanocomposites. The collaborative evidence from these analytical techniques strengthens the credibility of the findings and provides a comprehensive understanding of IRMOF-3 distribution on the

 © 2025 The Author(s). Published by the Royal Society of Chemistry

Open Access Article. Published on 18 December 2024. Downloaded on 1/21/2026 1:24:38 AM.
This article is licensed under a Creative Commons Attribution-NonCommercial 3.0 Unported Licence.

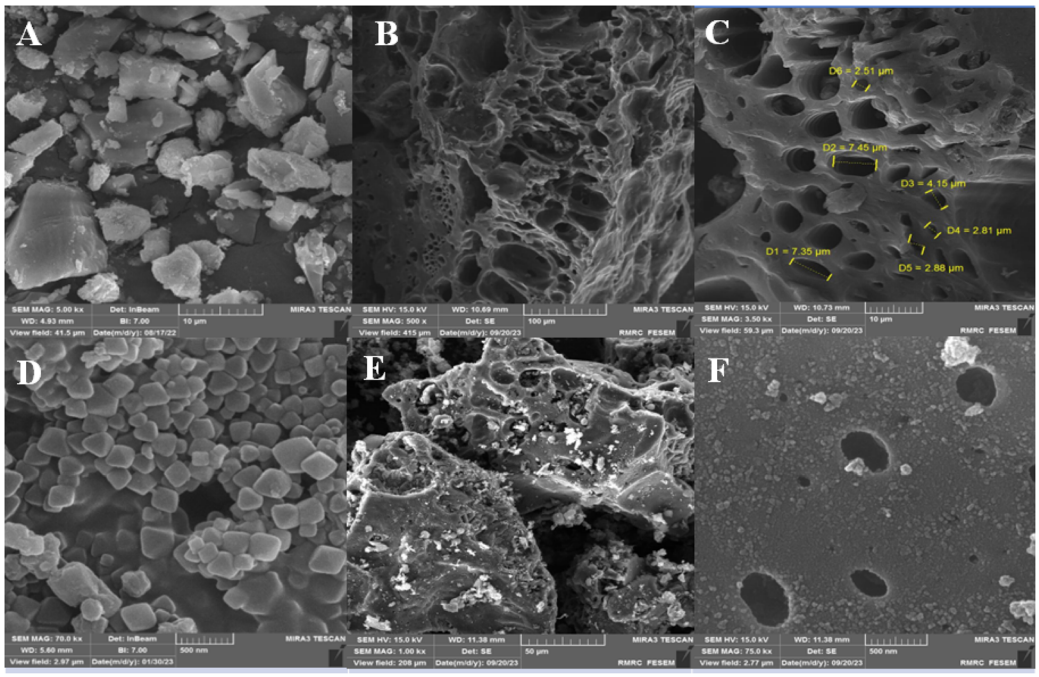

Fig. 5 FESEM images of raw material (Thymus leaves) (A), ACT (B and C), IRMOF-3 (D), ACT@IRMOF-3 (E and F).

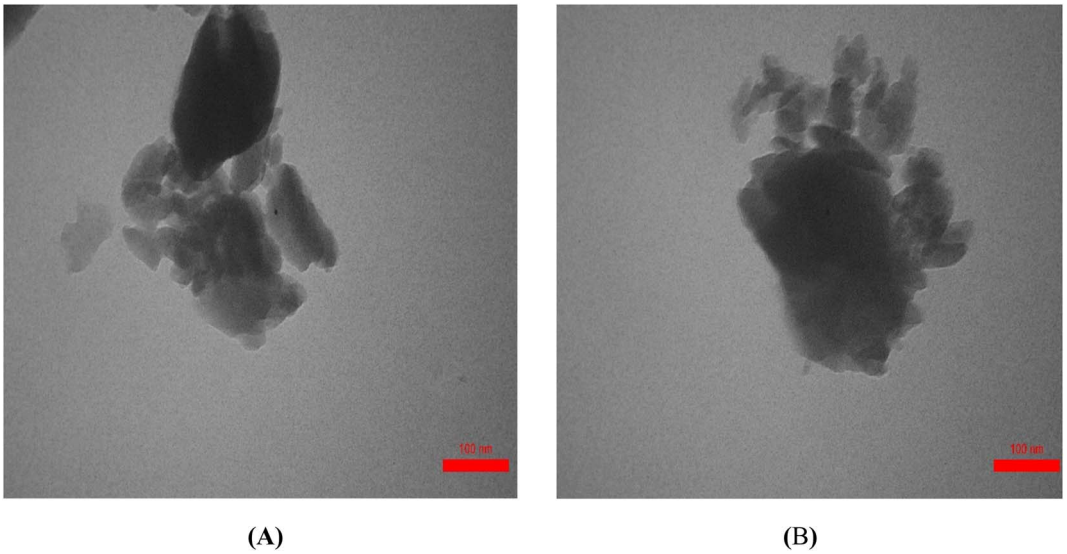

Fig. 6 TEM images of ACT@IRMOF-3 (A and B).

surface of CAT. The ACT@IRMOF-3 analysis reveals consistent distribution patterns of carbon, nitrogen, oxygen, and zinc elements. This indicates that ACT promotes the adsorption of IRMOF-3. By uniformly dispersing zinc as the active component in this heterogeneous catalyst, an increase in the number of active sites is anticipated to provide in a higher production rate of organic products.

To obtain specific surface area, nitrogen uptake and desorption, and total pore volume analysis was performed at 77 K (Fig. 9). The synthesized samples showed a combination of type III and IV isotherms, indicating a mesoporous structure.[28] The results show that ACT possesses a total specific surface area of 42.662 $m^2\ g^{-1}$, a pore size distribution of 54.52 Å, and a pore volume of 0.019 $cm^3\ g^{-1}$ (Fig. 9a, Table 1). The nitrogen adsorption/desorption isotherms of ACT@IRMOF-3 reveal a total specific surface area of 806 $m^2\ g^{-1}$, a pore size distribution of 1.22 nm, and a pore volume of 190.23 $cm^3\ g^{-1}$ (Fig. 9b, Table 1). The observed increase is related to the modification of ACT with IRMOF-3 NPs and the interaction of IRMOF-3 groups with the surface of ACT. The mesoporous structure is essential in effectively enhancing the catalytic activity in the ACT@IRMOF-3 matrix.

Open Access Article. Published on 18 December 2024. Downloaded on 1/21/2026 1:24:38 AM.
This article is licensed under a Creative Commons Attribution-NonCommercial 3.0 Unported Licence.

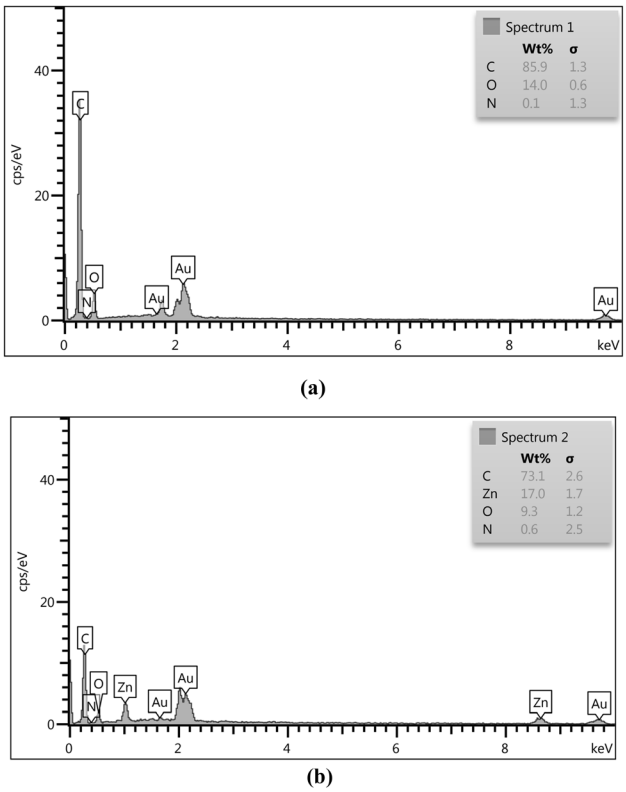

Fig. 7 EDS spectrum of ACT (a), and ACT@IRMOF-3 (b).

Fig. 10a indicates that ACT lost 12.06% of its weight in a two-step decomposition at 89.16 °C, and 340.04 °C in the order of their appearance (Fig. 10a). In the TGA curve of synthesized nanocatalyst, ACT@IRMOF-3 occurs *via* three successive steps (at 73.66 °C, 107.84 °C, and 306.25 °C), by which its losses are 25.58% of its weight (Fig. 10b). These results indicate that ACT@IRMOF-3 demonstrates high thermal stability compared to ACT. In addition, these analyses confirm the successful synthesis of ACT and ACT@IRMOF-3 nanocomposites.

Catalytic performance

Following the successful characterization of the activated carbon derived from Thymus plant (ACT) and ACT@IRMOF-3 our focus shifted towards investigating the optimum condition of the model reaction. For this preliminary study, we selected 1,2-phenylenediamine, dimedone, and benzaldehyde as reactants, and the experimental parameters were meticulously controlled (Table 2). Some parameters were studied to recognize the appropriate conditions for this reaction. The desired product was not synthesized in the absence of ACT@IRMOF-3 catalyst (entry 1). Therefore, the results indicate the pivotal catalytic role played by ACT@IRMOF-3 nanocomposite. Therefore, the experiment was done using different amounts of catalysts to found the effective amount of catalyst (entries 2–4). The best result was achieved when employing 5 mg of ACT@IRMOF-3 catalyst (entry 3) and produced yields of 95%. Increasing the catalyst dosage beyond 5 mg did not boost the reaction productivity (entry 4). The effectiveness of the

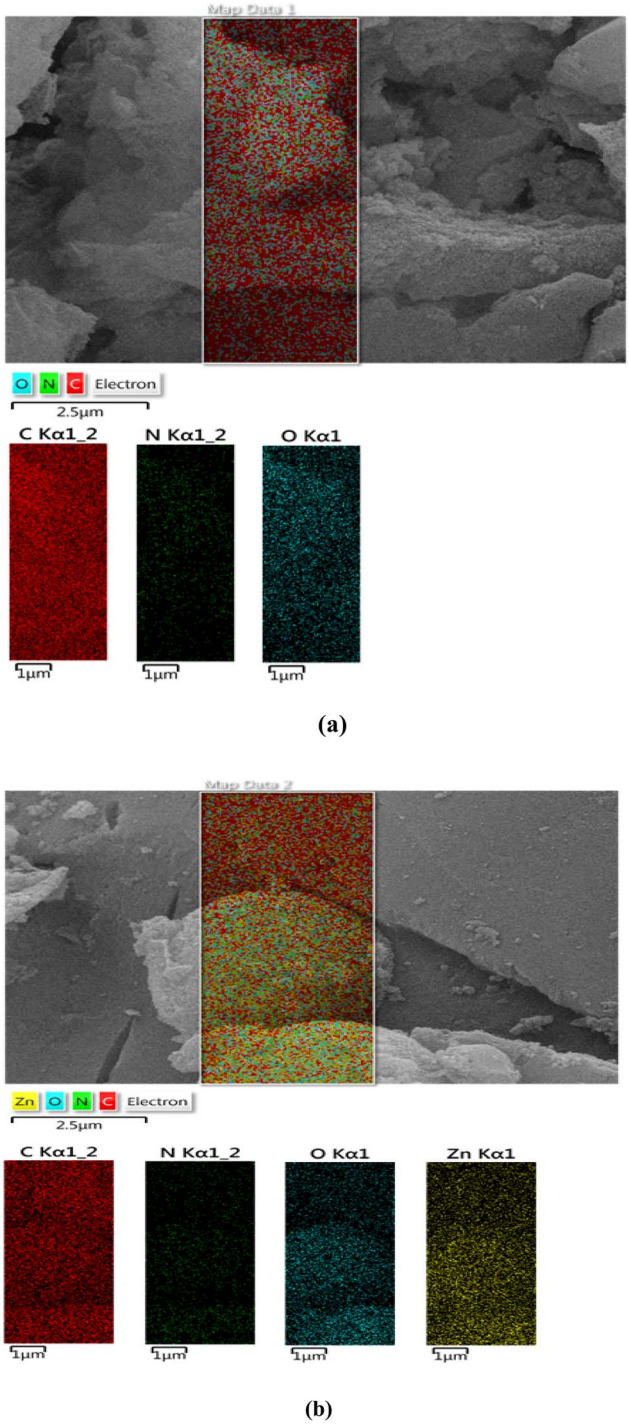

Fig. 8 Elemental mapping of ACT (a), and ACT@IRMOF-3 (b).

reaction was not enhanced by different temperatures such as room temperature and 60 °C (entries 5 and 6).

In addition, we performed experiments to investigate different solvents for the model reaction (entries 7–12). When the reaction was tested in water, the yield of the corresponding product went down. This is likely because some of the raw materials did not dissolve and there were fewer collisions and interactions between the raw materials, which are needed to

 © 2025 The Author(s). Published by the Royal Society of Chemistry

Open Access Article. Published on 18 December 2024. Downloaded on 1/21/2026 1:24:38 AM.
This article is licensed under a Creative Commons Attribution-NonCommercial 3.0 Unported Licence.

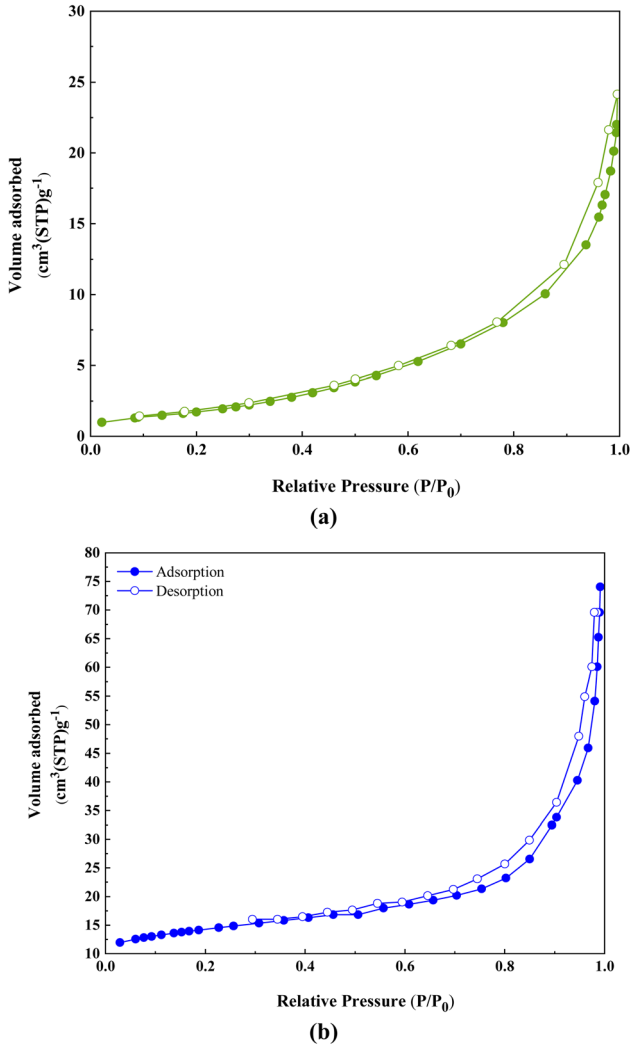

Fig. 9 N_2 adsorption–desorption of ACT (a), ACT@IRMOF-3 (b).

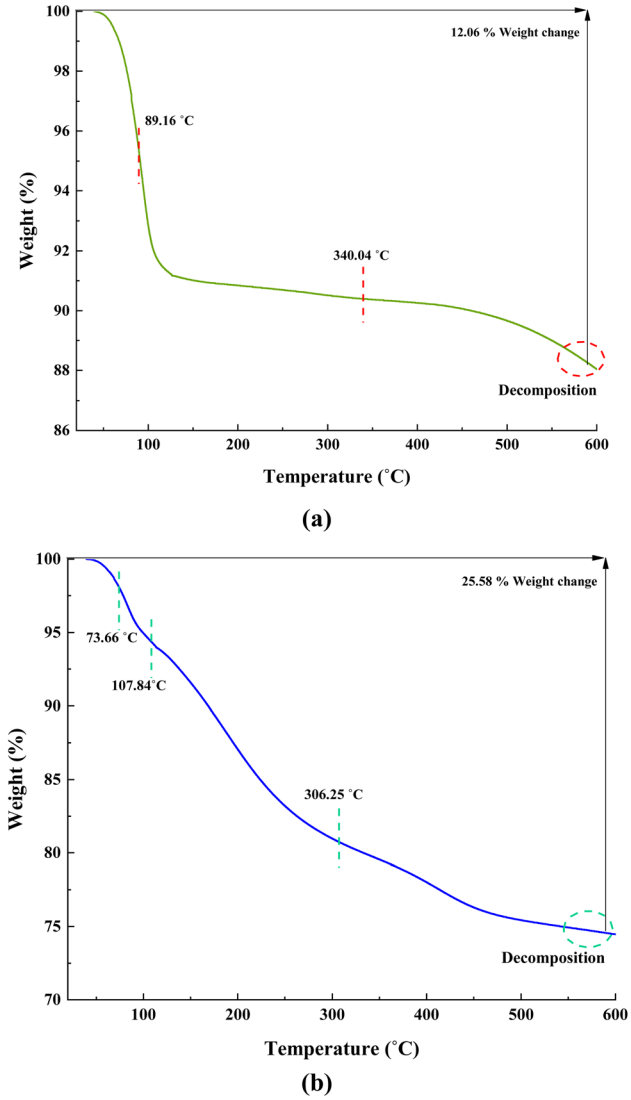

Fig. 10 TGA analysis of ACT (a), and ACT@IRMOF-3 (b).

Table 1 Langmuir and BET measurements results

Parameter	ACT	ACT@IRMOF-3
a_s (m^2 g^{-1})	42.662	806
V_m (cm^3(STP) g^{-1})	0.019	190.23
r_p	54.52 Å	1.22 nm
a_p (m^2 g^{-1})	13.86	6.5

turn them into intermediates and the corresponding products. The results showed that both methanol and PEG are good solvents for these organic transformations. On the contrary, there are problems in using these solvents, *i.e.*, the need for more purification steps, making this method less effective and less cost effective. Among these, ethanol proved to be the most effective solvent, resulting in the highest product yields. The excellent catalytic performance of the ACT@IRMOF-3 in the ethanol can be attributed to ACT@IRMOF-3's amphiphilic behavior using hydrophobic monomers (aromatic groups of ACT) and hydrophilic monomers (*i.e.*, Zn, carboxylate, and amine). Further, ACT@IRMOF-3 activates the intermediates *via* H-bonding with ACT@IRMOF-3's polar functional groups. It is worth noting that the presence of DMF, chloroform, PEG, and toluene solvents had a negative impact on the reaction efficiency. Furthermore, our investigation into different reaction times revealed that a duration of 60 minutes resulted in the highest conversion rate (entries 13 and 14).

Furthermore, we conducted a comparison of the efficiency between the ACT@IRMOF-3 catalyst and several catalyst precursors, including UiO-66-NH_2, MIL-101-NH_2 (Fe), IRMOF-3, MIL-101-NH_2 (Cr), and ACT. The best result was obtained when ACT@IRMOF-3 was utilized, as shown in Table 3, entries 1–6. This observation emphasizes the distinctive catalytic efficiency of ACT@IRMOF-3 in facilitating this particular organic transformation. By providing a platform for adsorption and reaction sites, activated carbon facilitates the conversion of reactants into desired products with enhanced efficiency. Moreover, IRMOF-3 accelerate the reaction by activating aldehydes and dimedone.

Open Access Article. Published on 18 December 2024. Downloaded on 1/21/2026 1:24:38 AM.
This article is licensed under a Creative Commons Attribution-NonCommercial 3.0 Unported Licence.

Table 2 Model reaction optimizations[a]

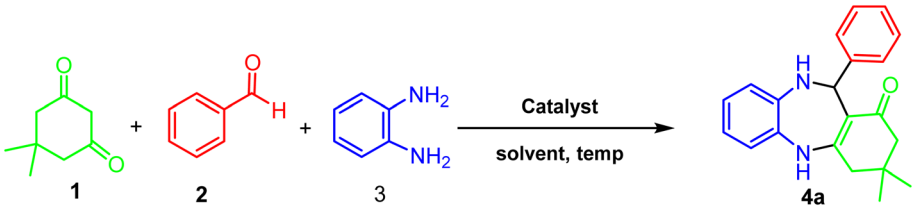

Entry	Cat. (mol%)	T (°C)	Solvent	Time (h)	Yield[b] (%)	TOF[c]	TON[d]
1	—	Reflux	EtOH	1	N. R.	—	—
2	ACT@IRMOF-3 (0.8)	Reflux	EtOH	1	75	93.75	93.75
3	ACT@IRMOF-3 (1.5)	Reflux	EtOH	1	95	63.33	63.33
4	ACT@IRMOF-3 (3)	Reflux	EtOH	1	95	31.66	31.66
5	ACT@IRMOF-3 (1.5)	—	EtOH	1	Trace	—	—
6	ACT@IRMOF-3 (1.5)	60 °C	EtOH	1	72	48	48
7	ACT@IRMOF-3 (1.5)	Reflux	H_2O	1	42	28	28
8	ACT@IRMOF-3 (1.5)	Reflux	MeOH	1	76	50.66	50.66
9	ACT@IRMOF-3 (1.5)	Reflux	DMF	1	57	38	38
10	ACT@IRMOF-3 (1.5)	Reflux	CHCl3	1	50	33.33	33.33
11	ACT@IRMOF-3 (1.5)	Reflux	PEG	1	53	35.33	35.33
12	ACT@IRMOF-3 (1.5)	Reflux	Toluene	1	35	29.16	29.16
13	ACT@IRMOF-3 (1.5)	Reflux	EtOH	2	95	31.66	63.33
14	ACT@IRMOF-3 (1.5)	Reflux	EtOH	0.5	58	77.33	38.66

[a] Reaction conditions: benzaldehyde (1 mmol), dimedone (1 mmol), 1,2-phenylenediamine (1 mmol), and ACT@IRMOF-3 nanocomposite. [b] Isolated yield. [c] TON = yield/amount of catalyst (mol). [d] TOF = TON/reaction time (h).

Table 3 Comparison efficiency of ACT@IRMOF-3 with different catalysts for the synthesis of **4a**

Entry	Catalyst (mg)	Condition	Solvent	Time (h)	Yield (%)
1	IRMOF-3 (5 mg)	Reflux	EtOH	1	70
2	ACT (5 mg)	Reflux	EtOH	1	40
3	UiO-66-NH_2 (5 mg)	Reflux	EtOH	1	60
4	MIL-101-NH_2 (Fe) (5 mg)	Reflux	EtOH	1	42
5	MIL-101-NH_2 (Cr) (5 mg)	Reflux	EtOH	1	35
6	ACT@IRMOF-3 (5 mg)	Reflux	EtOH	0.5	95

Following the successful attainment of both satisfactory and optimal catalytic performance from ACT@IRMOF-3, an in-depth exploration of its applicability across a diverse range of substrates is detailed in Table 4. The synthesized ACT@IRMOF-3 nanocatalyst exhibited notable strength in catalyzing the reaction involving aryl benzaldehyde as delineated in Table 4. The reactivity of diverse benzaldehydes with substituents (*p*-Cl, *p*-Br, *p*-NO_2, 2,4-Cl_2, *p*-$N(CH_3)_2$, *p*-OCH_3, *p*-CH_3, *p*-OH, *o*-OCH_3, H) was initiate to be moderate to good for producing the products. Aromatic diamines such as 1,2-phenylenediamine and 4-methylbenzene-1,2-diamine showed high yields of product. Especially remarkable was the fact that, compared to electron-donating-substituted substrates, electron-withdrawing groups on the aryl ring produced greater yields of the desired product in a short reaction time. Across this expansive spectrum of substrates, the reactions exhibited robust efficiency yielding a diverse array of products **4a–o**. Moreover, the reaction of aryl aldehydes with electron-donating groups (Me, OMe, OH, $N(Me)_2$) affects the aryl ring and prolongs the reaction time.

The yields ranged from 85% to 95%, underscoring the versatility of our methodology across a broad range of electron-rich and electron-deficient aryl benzaldehydes. This comprehensive investigation not only broadens the scope of applicable substrates but also showcases the adaptability of our approach to various chemical environments.

Proposed reaction mechanism

The mechanism takes place through the iminium route where the nucleophilic attack of 1,2-phenylenediamine to the dimedone activated by the Brønsted acid sites (–COOH group) of the carboxylic Zn-functionalized MOF catalyst form a C–N bond to give the intermediate **A**. The formed intermediate reacts with the benzaldehyde under similar reaction conditions on the Lewis acidic metallic nodes of Zn^{2+} to produce intermediate **B** as an intermediate iminium moiety. Additionally, the complexation of the imine group with Zn^{2+} increases the electrophilicity, facilitating the attack on enamine carbon to imine carbon, resulting in

 © 2025 The Author(s). Published by the Royal Society of Chemistry

Open Access Article. Published on 18 December 2024. Downloaded on 1/21/2026 1:24:38 AM.
This article is licensed under a Creative Commons Attribution-NonCommercial 3.0 Unported Licence.

Table 4 Synthesis of benzodiazepine derivatives using ACT@IRMOF-3[a]

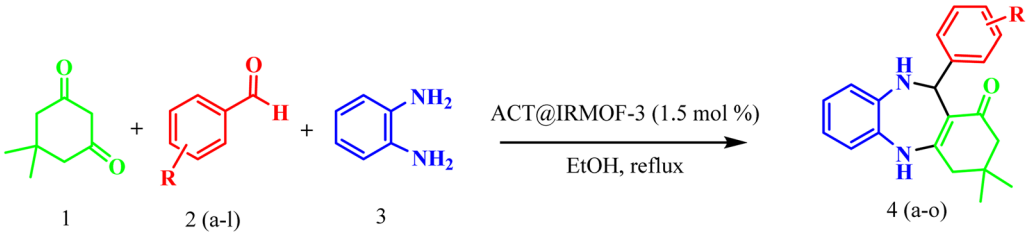

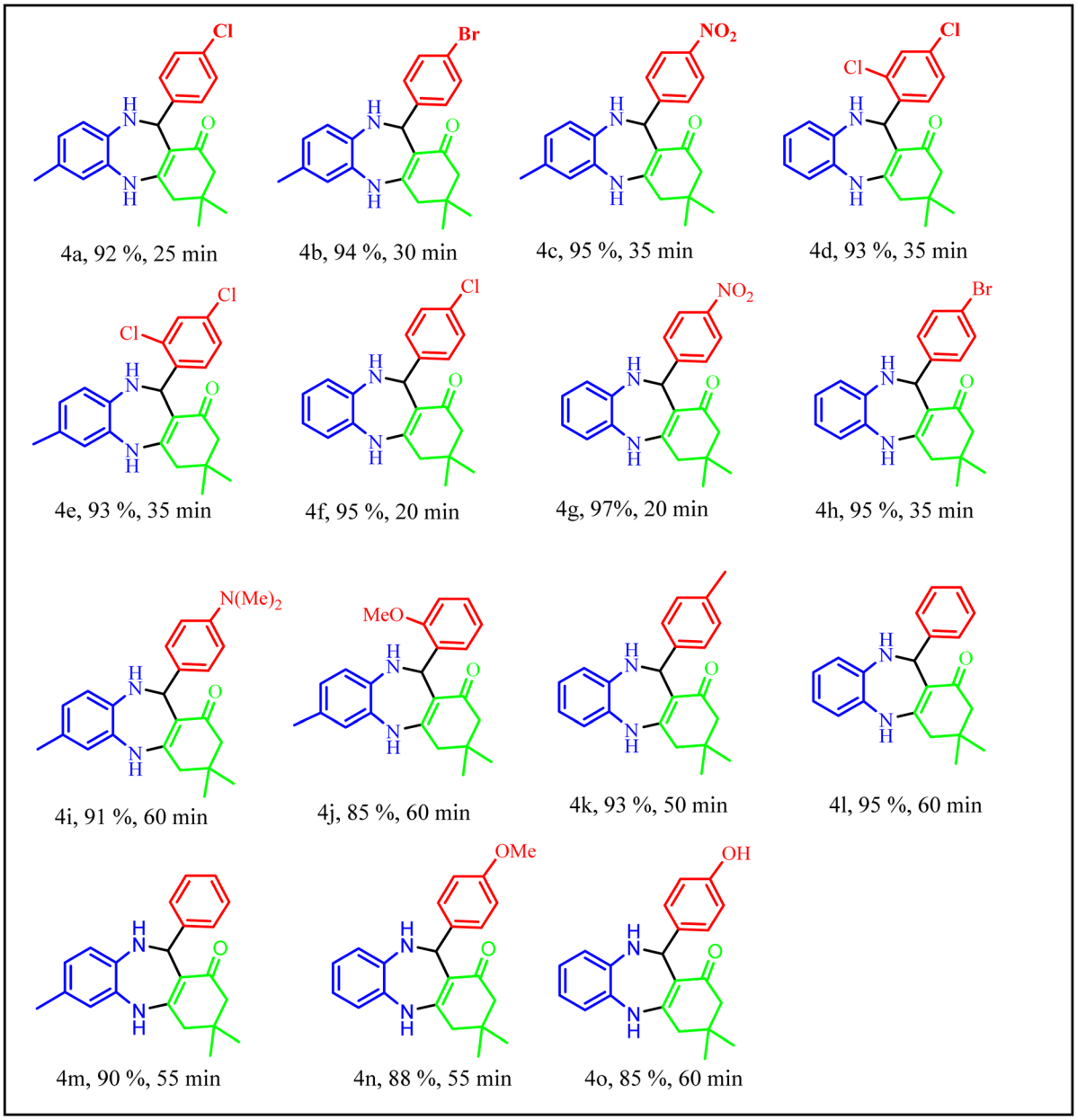

[a] Reaction conditions: benzaldehyde (1 mmol), dimedone (1 mmol), 1,2-phenylenediamine (1 mmol), and ACT@IRMOF-3 (1.5 mol%) in EtOH (2 mL) were heated at reflux condition.

the construction of seven-membered heterocyclic intermediate **C** with the help of Brønsted acid sites of the catalyst, which on dehydration provides the corresponding dihydropyrimidones the ACT@IRMOF-3 have a large number of both Lewis acidic Zn(II) center and Brønsted acid sites (–COOH group), which offer exceptional catalytic performance (Scheme 2).[32]

Open Access Article. Published on 18 December 2024. Downloaded on 1/21/2026 1:24:38 AM.
This article is licensed under a Creative Commons Attribution-NonCommercial 3.0 Unported Licence.

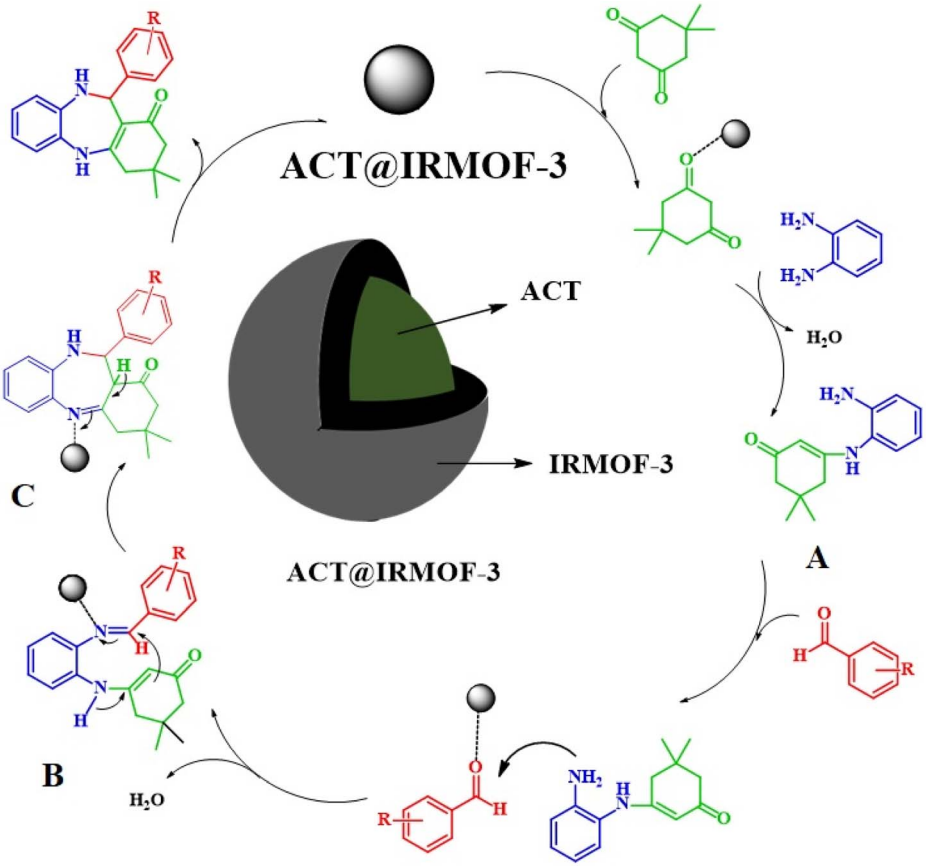

Scheme 2 The proposed mechanism for the synthesis of benzodiazepine using ACT@IRMOF-3.

Comparison study

To show the method efficiency in the synthesis of benzodiazepines, the product **4a** were compared with other reported methods (Table 5). The ACT@IRMOF-3 nanocomposite (1.5 mol%, 5 mg) outperforms the other nanocomposites in both reaction time and yield. It is valuable to know that activated carbon, and IRMOF-3, are biodegradable and environmentally friendly with high loading capacity to reduce the amount of catalyst needed for the reaction (entry 5).

Recovery and reusability

The recyclability of heterogeneous catalysts presents significant advantages in terms of both economics and sustainability. In this context, we conducted a thorough investigation into the potential for recycling and reusing IRMOF-3 immobilized on activated carbon of thymus ACT@IRMOF-3. To evaluate the recyclability of ACT@IRMOF-3, the optimal conditions were employed to re-examine the reaction between 4-chlorobenzaldehyde and dimedone with 1,2-phenylenediamine. Following the initial reaction cycle, the reaction mixture underwent dilution with ethanol. Subsequently, the reaction vial underwent centrifugation, effectively separating the ethanol layer. This process was iterated, and the spent ACT@IRMOF-3 was then dried at 80 °C for subsequent use under identical conditions. Impressively, ACT@IRMOF-3 displayed notable durability, enabling its reuse across six consecutive cycles without a significant decrease in catalytic performance (95, 95, 93, 91, 88, and 85%). FESEM analysis, as depicted in Fig. 11, confirms the integrity of the IRMOF-3 species and their non-

Table 5 Comparison of this work with the reported works in the reaction of 4-chlorobenzaldehyde, dimedone, and 1,2-phenylene diamine

Entry	Catalyst	Solvent	T (°C)	Time (min)	Yield (%)	Ref.
1	$CoFe_2O_4$@GO–Kryptofix 22	Solvent-free	60	15	87	31
2	ZnS NPs	EtOH	Reflux	19	85	33
3	Chitosan functionalized by triacid imide	EtOH	Rt	40	93	34
4	CuO@Nitrogen graphene quantum Dots@NH_2	EtOH	Rt	30	94	34
5	ACT@IRMOF-3	EtOH	Reflux	20	95	This work

 © 2025 The Author(s). Published by the Royal Society of Chemistry

Open Access Article. Published on 18 December 2024. Downloaded on 1/21/2026 1:24:38 AM.
This article is licensed under a Creative Commons Attribution-NonCommercial 3.0 Unported Licence.

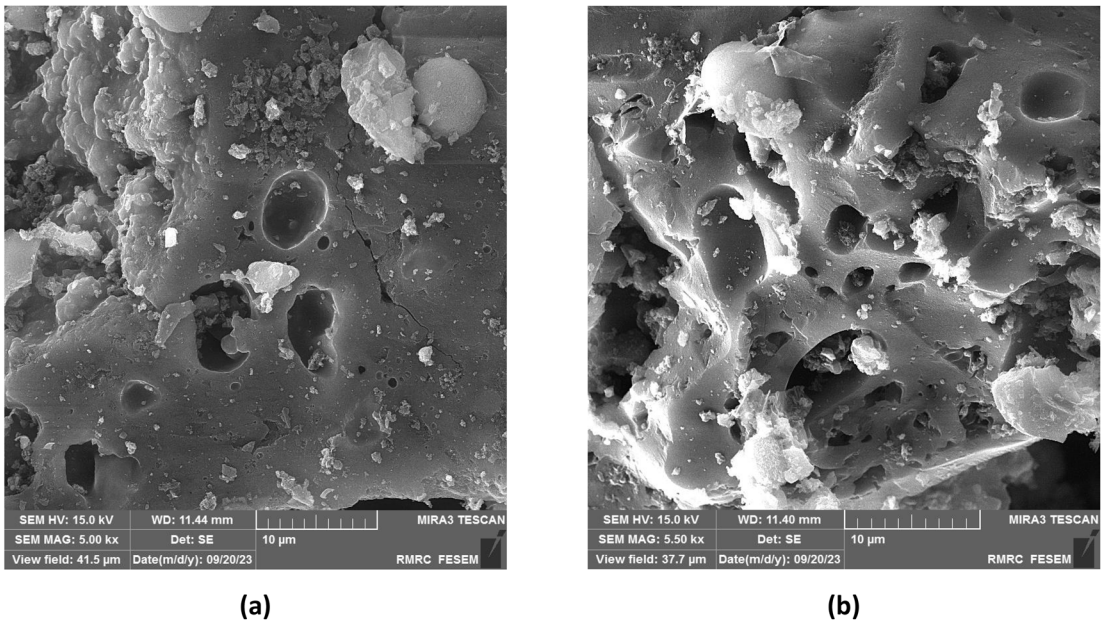

Fig. 11 FESEM of recycled ACT@IRMOF-3 nanocatalyst after six times at the scale bare of 10 μm (a and b).

aggregation during the catalytic cycles. It is noteworthy that the marginal reduction in catalytic efficiency observed may be linked to the loss of ACT@IRMOF-3 during the centrifugation process. The FT-IR analysis of the recycled catalyst demonstrates its excellent chemical stability (Fig. 12).

Hot-filtration and leaching test

The experiment conducted included a hot-filtration test and a leaching analysis on a model chemical reaction (product **4l**). Following 30 minutes, the reaction mixture was diluted with EtOH (3 mL), and the ACT@IRMOF-3 catalyst was separated using a centrifugation process. The separated liquid component was then returned to the oil bath to react for an additional 30 min. It was noted that the product yield did not significantly increase beyond 45%. These findings indicate that the catalyst (ACT@IRMOF-3) exhibits heterogeneous behavior.

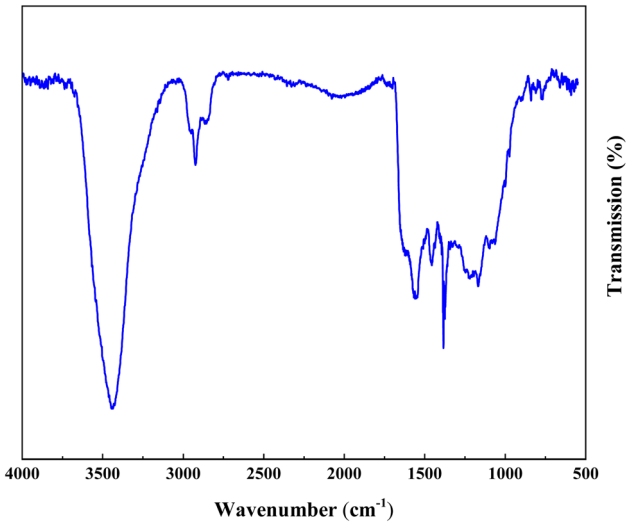

Fig. 12 FTIR of recycled ACT@IRMOF-3 nanocatalyst after six times.

Conclusions

ACT@IRMOF-3 nanohybrid containing activated carbon, and IRMOF-3 was synthesized for the selective synthesis of benzodiazepines. The development of this recyclable activated carbon-modified IRMOF-3 nanocatalyst represents a significant step towards sustainable and efficient catalysis. It offers a promising solution for the synthesis of benzodiazepines, reducing the environmental impact, and costs associated with traditional catalytic methods. A synergistic effect is produced in the production of benzodiazepines by the special combination of IRMOF-3 with activated carbon. In general, the ACT@IRMOF-3 nanocatalyst presented in this study offers advantages, such as simple preparation, broad reaction versatility, long cycle times, high target product yields, and minimal environmental impact. This work indicates that ACT@IRMOF-3 core–shell could be applied as excellent nanocatalyst in organic synthesis due to the high surface area and economical synthesis method. According to growing interest in mesoporous carbon-based nanocatalysis, it is anticipated that such catalyst systems will find widespread use in various organic syntheses.

Data availability

Data is provided within the manuscript or ESI.†

Conflicts of interest

There are no conflicts to declare.

Open Access Article. Published on 18 December 2024. Downloaded on 1/21/2026 1:24:38 AM.
This article is licensed under a Creative Commons Attribution-NonCommercial 3.0 Unported Licence.

Acknowledgements

The authors wish to thank Bu-Ali Sina University, Center of Excellence Developmental of Environmentally Friendly Methods for Chemical Synthesis (CEDEFMCS) for financial support in carrying out this research.

References

1 S. Rashki, *et al.*, Chitosan-based nanoparticles against bacterial infections, *Carbohydr. Polym.*, 2021, **251**, 117108.
2 A. L. Jarallah and A. F. Kareem, Synthesis, Examination of Various Seven Rings, and Effects on Corrosion and Fungus, *J. Med. Chem.*, 2023, **6**(3), 532–539.
3 E. Sanabria, R. E. Cuenca, M. Esteso and M. Maldonado, Benzodiazepines: Their Use either as Essential Medicines or as Toxics Substances, *Toxics*, 2021, **9**(2), 25.
4 R. Taghavi and S. Rostamnia, Four-Component Synthesis of Polyhydroquinolines *via* Unsymmetrical Hantzsch Reaction Employing Cu-IRMOF-3 as a Robust Heterogeneous Catalyst, *Chem. Methodol.*, 2022, **6**(9), 639–648.
5 A. V. da Silva, S. M. P. Meneghetti and M. R. Meneghetti, Benzodiazepines: Drugs with Chemical Skeletons Suitable for the Preparation of Metallacycles with Potential Pharmacological Activity, *Molecules*, 2021, **26**(9), 2796.
6 M. Ivanova, T. Poisson, P. Jubault and J. Legros, Flow platform for the synthesis of benzodiazepines, *J. Flow Chem.*, 2023, **13**(1), 45–52.
7 S. Tao, Q. Bu, Q. Shi, D. Wei, B. Dai and N. Liu, Synthesis of Benzodiazepines Through Ring Opening/Ring Closure of Benzimidazole Salts, *Chem.–Eur. J.*, 2020, **26**(15), 3252–3258.
8 P. Bhardwaj and N. Kaur, Synthesis of 1, 4-Benzodiazepines by Palladium-Catalyzed CN Coupling, *Curr. Org. Chem.*, 2023, **27**(4), 282–296.
9 H. Farhid, V. Khodkari, M. T. Nazeri, S. Javanbakht and A. Shaabani, Multicomponent reactions as a potent tool for the synthesis of benzodiazepines, *Org. Biomol. Chem.*, 2021, **19**(15), 3318–3358, DOI: 10.1039/D0OB02600J.
10 S. Heidari, S. Alavinia and R. Ghorbani-Vaghei, Green synthesis of thiourea derivatives from nitrobenzenes using Ni nanoparticles immobilized on triazine-aminopyridine-modified MIL-101(Cr) MOF, *Sci. Rep.*, 2023, **13**(1), 12964.
11 V. Izadkhah, R. Ghorbani-Vaghei, S. Alavinia, S. Asadabadi, N. Emami and S. Jamehbozorgi, Fabrication of zirconium metal-organic-framework/poly triazine-phosphanimine nanocomposite for dye adsorption from contaminated water: Isotherms and kinetics models, *J. Mol. Struct.*, 2023, **1275**, 134691.
12 S. Koosha, S. Alavinia and R. Ghorbani-Vaghei, CuI nanoparticles-immobilized on a hybrid material composed of IRMOF-3 and a sulfonamide-based porous organic polymer as an efficient nanocatalyst for one-pot synthesis of 2,3-disubstituted benzo[*b*]furans, *Arabian J. Chem.*, 2023, **16**(8), 104975.
13 M. Yaghubzadeh, S. Alavinia and R. Ghorbani-Vaghei, A sustainable protocol for selective alcohols oxidation using a novel iron-based metal organic framework (MOF-BASU1), *RSC Adv.*, 2023, **13**(35), 24639–24648, DOI: 10.1039/D3RA03058J.
14 S. Sharafinia, A. Farrokhnia and E. G. Lemraski, The adsorption of cationic dye onto ACPMG@ZIF-8 core-shell, optimization using central composite response surface methodology (CCRSM), *Colloids Surf., A*, 2022, **634**, 128039.
15 J. Babamoradi, R. Ghorbani-Vaghei and S. Alavinia, Click synthesis of 1,2,3-triazoles using copper iodide nanoparticles anchored poly(sulfonamide-thiazole) modified layered double hydroxides/chitosan nanocomposite, *Int. J. Biol. Macromol.*, 2022, **209**, 1542–1552.
16 R. Ghiai, S. Alavinia, R. Ghorbani-Vaghei, A. Khazaei, R. Karimi-Nami and I. Karakaya, Synthesis of benzothiazoles using an iron-anchored polysulfonamide modified layered double oxide/sodium alginate nanocomposite, *J. Mater. Chem.*, 2024, **12**(9), 5474–5492, DOI: 10.1039/D3TA06022E.
17 S. Solgi, R. Ghorbani-Vaghei and S. Alavinia, Application of copper iodide nanoparticles immobilized porous polysulfonamide gel as an effective nanocatalyst for synthesis of aminoindolizines, *J. Porous Mater.*, 2021, **28**(1), 289–298.
18 V. B. Jaryal, A. Villa and N. Gupta, Metal-Free Carbon-Based Nanomaterials: Insights from Synthesis to Applications in Sustainable Catalysis, *ACS Sustain. Chem. Eng.*, 2023, **11**(41), 14841–14865.
19 N. Rodoshi Khan and A. Bin Rashid, Carbon-Based Nanomaterials: a Paradigm Shift in Biofuel Synthesis and Processing for a Sustainable Energy Future, *Energy Convers. Manage.:X*, 2024, **22**, 100590.
20 P. Chaudhary, S. Bansal, B. B. Sharma, S. Saini and A. Joshi, Waste biomass-derived activated carbons for various energy storage device applications: A review, *J. Energy Storage*, 2024, **78**, 109996.
21 S. Sharafinia, A. Farrokhnia and E. G. Lemraski, The adsorption of cationic dye onto ACPMG@ZIF-8 core-shell, optimization using central composite response surface methodology (CCRSM), *Colloids Surf., A*, 2022, **634**, 128039.
22 N. Shekarlab, R. Ghorbani-Vaghei and S. Alavinia, Preparation and characterization of copper/polysulfonamide complex immobilized on graphene oxide as a novel catalyst for the synthesis of pyrimido[1,2-*a*]benzimidazoles, *Appl. Organomet. Chem.*, 2020, **34**(11), e5918.
23 D. Sharma, P. Choudhary, S. Kumar and V. Krishnan, Interfacial nanoarchitectonics of nickel phosphide supported on activated carbon for transfer hydrogenation of nitroarenes under mild conditions, *J. Colloid Interface Sci.*, 2024, **657**, 449–462.
24 J. Qin, *et al.*, Polymerization synthesis of semi-coke activated carbon modified carbon nitride nanoscrolls with boosted photocatalytic H2 production, *J. Mol. Catal.*, 2024, **556**, 113918.
25 S. M. Marvast and E. Rostami, Graphene Oxide Modified with Tetramethylethylenediamine Ammonium Salt as a Powerful Catalyst for Production of Trisubstituted Imidazoles, *Asian J. Green Chem.*, 2024, **8**(3), 261–277.

 © 2025 The Author(s). Published by the Royal Society of Chemistry

Open Access Article. Published on 18 December 2024. Downloaded on 1/21/2026 1:24:38 AM.
This article is licensed under a Creative Commons Attribution-NonCommercial 3.0 Unported Licence.

26 E. G. Lemraski and S. Sharafinia, Kinetics, equilibrium and thermodynamics studies of Pb2+ adsorption onto new activated carbon prepared from Persian mesquite grain, *J. Mol. Liq.*, 2016, **219**, 482–492.

27 S. Koosha, S. Alavinia and R. Ghorbani-Vaghei, CuI nanoparticles-immobilized on a hybrid material composed of IRMOF-3 and a sulfonamide-based porous organic polymer as an efficient nanocatalyst for one-pot synthesis of 2,3-disubstituted benzo[*b*]furans, *Arabian J. Chem.*, 2023, **16**(8), 104975.

28 J. Babamoradi, S. Alavinia, R. Ghorbani-Vaghei and R. Azadbakht, Catalytic application of a novel melamine–naphthalene-1, 3-disulfonic acid metal–organic framework in the synthesis of β-acetamido ketones, *New J. Chem.*, 2022, **46**(48), 23394–23403.

29 S. Koosha, S. Alavinia and R. Ghorbani-Vaghei, CuI nanoparticle-immobilized on a hybrid material composed of IRMOF-3 and a sulfonamide-based porous organic polymer as an efficient nanocatalyst for one-pot synthesis of 2,4-diaryl-quinolines, *RSC Adv.*, 2023, **13**(17), 11480–11494, DOI: **10.1039/D3RA01164J**.

30 S. Koosha, S. Alavinia and R. Ghorbani-Vaghei, CuI nanoparticle-immobilized on a hybrid material composed of IRMOF-3 and a sulfonamide-based porous organic polymer as an efficient nanocatalyst for one-pot synthesis of 2, 4-diaryl-quinolines, *RSC Adv.*, 2023, **13**(17), 11480–11494.

31 M. Esfandiari, A. K. Abbas, M. R. Vakili, H. Shahbazi-Alavi and J. Safaei-Ghomi, Synthesis of benzodiazepines catalyzed by chitosan functionalized by triacid imide as a superior catalyst, *Res. Chem. Intermed.*, 2021, **47**(2), 483–496.

32 M. Esfandiari, A. Kareem Abbas, H. Shahbazi-Alavi and J. Safaei-Ghomi, Synthesis of Benzodiazepines Promoted by CeO2/CuO@Nitrogen Graphene Quantum Dots@NH_2 Nanocomposite, *Polycyclic Aromat. Compd.*, 2022, **42**(4), 1235–1248.

33 R. Mozafari and M. Ghadermazi, A nickel nanoparticle engineered $CoFe_2O_4$@GO–Kryptofix 22 composite: a green and retrievable catalytic system for the synthesis of 1,4-benzodiazepines in water, *RSC Adv.*, 2020, **10**(26), 15052–15064, DOI: **10.1039/D0RA01671C**.

34 H. Naeimi and H. Foroughi, Facile three-component preparation of benzodiazepine derivatives catalyzed by zinc sulfide nanoparticles *via* grinding method, *Res. Chem. Intermed.*, 2016, **42**(5), 3999–4020.